



An official publication of the International Society for Energy, Environment and Sustainability (ISEES)

Journal of Energy and Environmental Sustainability

Journal homepage : www.jees.in

Subcooled Pool Boiling on Ultra-thin Strips of Varying Cross-sections

Amrita Birhman^a, Sanjid C S^a, John Pinto^a, Anuj Sethia^a, Janani Srree Murallidharan^{a*}^aDepartment of Mechanical Engineering, Indian Institute of Technology, Bombay 400076, India

ARTICLE INFO

Received : 07 October 2019
 Revised : 07 October 2019
 Accepted : 21 October 2019

Keywords:

Pool boiling, Bubble growth modelling,
 Subcooling, Varying cross-section

ABSTRACT

The Boiling heat transfer phenomenon can be used for effectively cooling microelectronic chips. However, since these systems belong to such small length scales, and are in various shapes and sizes, the boiling phenomenon will be different from that observed in macro systems. The present study looks into the fundamental similarities/differences in the phenomenon by studying the growth of bubbles on ultra-thin strips. An experimental investigation is conducted to generate bubbles of various sizes on a unique double dog-bone shaped thin substrate. The growth and departure of the bubble generated on various sections of the substrate were studied. The bubbles observed on these different sections of an identical substrate were found to have considerable interdependency. Additionally, data generated is for very high subcooling that is not available in the literature. Bubble growth and departure model was developed, and preliminary results indicate improved bubble departure prediction capabilities across a wide range of subcooling.

© 2019 ISEES, All rights reserved

Nomenclature

CHF	Critical heat flux
l	liquid
d	diameter
ML	evaporation through micro layer
F	Force
fps	frames per second
PB	evaporation from surrounding liquid
g	acceleration due to gravity
Ja	Jakob number
r	curvature at contact
K	Bubble growth
s	Surface tension force in vertical direction
Pr	Prandtl number
R	Bubble radius or surface roughness
sat	saturated
SHL	Super heated layer
v	vapour
T	Temperature
w	wall contact
	wall solid substrate (wall)
t	time

X	Subcooling factor
η	Thermal diffusivity
ρ	Density
σ	Surface tension coefficient
y	vertical component
1	First derivative with time
2	2 nd derivative with time

Subscripts

b	buoyancy
bulk	fluid bulk
c	contact
g	growth

1. Introduction

Boiling heat transfer has been a major topic of study for several decades due to the central role it plays in the heat transfer achieved by industrial systems like Pressurized Water Reactors (PWRs), etc. Its study has added importance, due to its capability to also trigger safety-crisis related events, such as the 'Critical Heat Flux' (CHF) condition. The CHF-like condition is mainly triggered by accumulation of bubbles at the heater surface, which results in a significant increase of local wall temperature, eventually

* Corresponding Author: : js.murallidharan@iitb.ac.in

leading to the system's failure. The importance of boiling heat transfer, and the CHF phenomenon, is not limited to large industrial systems, but is relevant even in the cooling of microelectronics. However, there will be a change in the phenomenon due to the difference in length scales. When dealing with microsystems, the small dimensions make additional heat transfer mechanisms such as axial conduction relevant, which is usually negligible in larger systems [Gupta et al., 2018]. Most studies thus far, have looked at boiling where the phenomenon is not influenced by the system's dimensions or its complex shapes. The present study is important in that its goal is to study and understand near-wall vapour dynamics on ultra-thin strips. More specifically, the goal is to study the bubble growth rate, as it is the growth of the bubble that governs the bubble departure size and frequency. This in turn will influence the amount of heat transfer that will be achieved at the surface. The changes in boiling heat transfer that will occur in such situations, and the ability to model it mathematically, will help in designing more safe and efficient microsystems.

2. Literature review

Relevant literature on experimental studies and mathematical modelling of subcooled pool boiling is presented in this section.

2.1 Experimental studies on pool boiling

Studies that look at boiling in microsystems are available; however they have been performed mainly for microchannel flow boiling conditions [Liang and Mudawar, 2019; Kim and Mudawar, 2014]. Micro-scale studies on bubble dynamics are also available, however, the focus there was to capture the minute dynamics of a bubble growing on uniform flat surfaces. The understanding gained from these studies was largely applied to boiling in macrosystems. In both these classes of studies, the bubble dynamics, bubble growth period, bubble departure diameter, and bubble release frequency were studied. Duan et al. [2013] used high speed imaging, IR thermometry, and PIV measurements to capture the bubble dynamics at various heat flux and superheat. Shen et al. [2015] created a mixed wettability surface by applying a coating of hydrophobic PTFE over TiO_2 to observe the decrease in waiting time between the successive bubbles. Kim et al. [2017] identified that a larger contact angle created from a relatively more hydrophobic surface result in a large diameter bubble, which helps it to leave the surface easily. These studies repeatedly emphasised that the parametric study of bubble dynamics is important in order to understand the nucleate boiling heat transfer and developed models describing the boiling, especially for macrosystems.

Fluid pressure affects the bubble growth rate and departure diameter to a great extent. There are several studies which relate the bubble diameter for pool boiling of water at atmospheric pressure to the same at lower pressure [Giraud et al., 2015; Michaie et al., 2017; Kowalewski et al., 2000]. Giraud et al. [2015] went to a pressure of 1.8 kPa to show that bubble diameter increases with decreasing pressure. According to the study, a bubble with the spherical shape of millimetre size changes to the mushroom shape of a few centimetres size in the sub atmospheric pressure.

Goel et al. [2017] had attempted to study the effect of various surface properties like roughness and inclination angle on bubble behaviour. They used the bubble departure diameters and frequencies to calculate the nucleate boiling heat flux by using some empirical relations derived from their experiments in the subcooled range up to 20 K. Hao et al. [2005] and Lu and Peng [2006] heated a micro-wire in the (40 -60 K) subcooled water and reported the leaping and slipping of bubbles. Thus, the review of the literature reveals that the formation of bubbles and their effect on the rate of heat transfer is a complex phenomenon, and depends on many parameters such as bulk temperature, working pressure, etc. It can also be seen that parametric dependence on some factors has been explored more than others. A very popular parameter is liquid subcooling, due to its role in achieving increased heat transfer. Several experiments on subcooled flow boiling have been performed [Goel et al., 2017]. However, microscale studies looking at bubble dynamics in subcooled pool boiling are sparse.

With the advent of new technology, microelectronics are becoming more flexible and are manufactured with complex shapes. There is absolutely no understanding in the literature of boiling on such complex-shaped microelectronic strips, where the varying cross-sections of the strips will affect the boiling characteristics. Moreover a review article by Gupta et al. [2018] shows the relevance of studies to be conducted on thin substrates. The length scales of the thin substrate are less than 0.1 mm. However, most boiling studies address larger length scales. In fact, boiling studies of Dhilon et al. [2015], have some of the smallest length scales. Their experiments were performed with a substrate thickness of 0.6 mm. In our study we are utilizing substrates that are thinner, i.e. with a thickness

of 0.1 mm. These dimensions were chosen to understand the bubble behaviour at length scales relevant to miniaturized electronics. In this study, experiments are performed to shed light on these aspects.

2.2 Modelling studies on bubble growth

Models for bubble departure and lift-off have been developed for a wide range of boiling conditions. Zeng et al. [1993] and Klausner et al. [1993] provided a force-balance based bubble departure model, for both pool and flow boiling. However, Zeng et al. [1993] model was only applicable for saturated liquid at elevated pressures as well as in microgravity conditions. Judd et al. [1991] developed a model to compute the boiling heat flux and incorporated within it, sub-models that compute the contributions of micro-layer evaporation, natural convection, and nucleate boiling. Sugrue et al. [2014] conducted experiments of subcooled flow boiling, at lower heat flux conditions, with different test section orientations. They concluded based on their study that surface tension and shear lift are the dominant forces influencing bubble departure. It is concluded that models calculating bubble growth and departure were mostly developed and tested for flow boiling conditions. More importantly, due to a lack of subcooled pool boiling data, there is no model that can model bubble growth and departure for both subcooled and saturated pool boiling conditions comprehensively.

Thus, from this literature review, it can be concluded that fundamental aspects of boiling in microsystems have still not been understood. Specifically, the effect of varying cross-sections, high subcooling, etc., on ultra-thin systems are yet unexplored. Due to the lack of experimental studies in this area, there is no mathematical model that can accurately predict subcooled pool boiling. The present paper tries to address this lacuna. It performs experiments at high subcooled conditions to study pool boiling from natural nucleation sites, using ultra-thin strips of varying cross-sections. As anticipated, different sized bubbles are formed, and this study looked into the fundamental similarities/differences between these bubbles. A preliminary version of a bubble departure model is also presented, which can predict both subcooled and saturation bubble departure for a wide range of pool boiling conditions.

3. Methodology

3.1 Experimental details

A schematic representation of the experimental setup used for the present investigation is provided in Figure 1a and its component description is provided here. The sample geometry was chosen to be a uniquely designed double dog-bone shape which creates different heat flux in the different sections of the sample with the same power input as shown in Figure 1b. The sample was placed in a cylindrical glass container (ϕ 200 mm x 100 mm) completely filled with distilled water and the desired bulk temperature was maintained using a separate 1 kW bulk heater. All the experiments were conducted at atmospheric pressure conditions. Only natural nucleation sites were focused for measurements. K type thermocouple was used to measure the bulk temperature of the water with an accuracy of $\pm 0.09^\circ\text{C}$. Visualization of bubbles was done using a Photron SA5 high speed camera at 50-1000 fps and a resolution of 1024 x 1024 pixels using a 90 mm f/2.8 Tamron Macro Lens. Bowens Gemini 1000 pro mono light was used as a light source. Various experiments were performed at different heat flux, and at different subcooling ranging from 20-65 K to capture the bubble dynamics.

Bubble diameter was predominantly measured. This was calculated by measuring the horizontal and vertical diameter from the optical images and by using the relation from Goel et al. [2017]. It was assumed that the bubble in contact with the sample surface had symmetry about the vertical axis. This assumption was validated by taking the measurements of a still bubble from different radial positions around the test setup. The images were calibrated prior to experiment.

Uncertainties: The resolution of the optical system (camera+lens) was 19.5 $\mu\text{m}/\text{px}$. For a bubble of 0.5 mm diameter, the uncertainty in the length scale was 4%, and for the bubble diameter of 1 mm, it was 2%. The power supply (model PSW 30-108 by Gwinstek) was used for supplying the power and measurement of current. For heat flux calculation, the current measurement resolution was 3 mA. For an experiment at 5 amp, the uncertainty was 0.06%.

3.2 Mathematical model

Bubble growth rate prediction is one of the most challenging parts in solving the bubble dynamics in both pool and flow boiling. Various factors affecting it are pressure, saturation temperature, liquid to vapour density ratio, the heat flux, mass flux, contact angles, wall temperature,

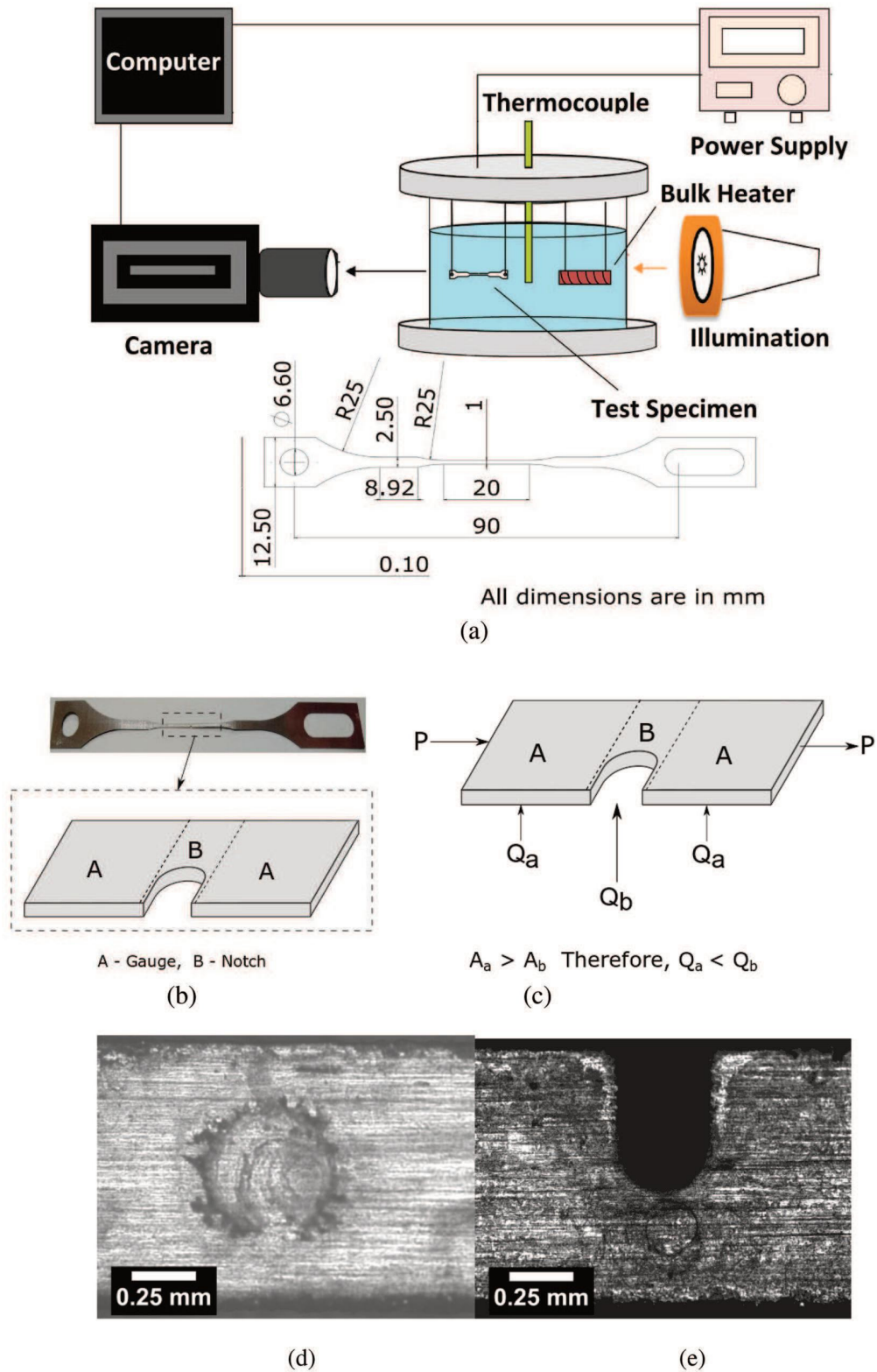


Figure 1: (a) Schematic representation of experimental setup, (b) photographic image of nichrome strip along with schematic representation of the Gauge and Notch section, (d) schematic representation of heat flux distribution along the strip cross-section, (e) burn marks appeared on notch and, (f) gauge section of the strip.

thermal boundary layer thickness, contact diameter, etc. All these parameters are incorporated into the present model, which is a modification of the model developed for flow boiling by Mazzocco et al. [2018]

$$K_{ML} = 2 \frac{\pi^{2.1}}{\pi^2} Ja^{2.1} \sqrt{\frac{\eta_l}{Pr_l \pi}} \quad (1)$$

$$K_{PB} = 2 \sqrt{\frac{3\eta_l}{\pi}} Ja^{2.125} \quad (2)$$

$$\chi = (T_{wall} - T_{sat}) / (T_{sat} - T_{bulk}) \quad (3)$$

$$R(t) = \chi(K_{ML} + K_{PB})t^{0.5} \quad (4)$$

where, K_{ML} is the growth due to the evaporation through micro-layer beneath the bubble and K_{PB} is the bubble growth due to the evaporation from the surrounding liquid. Ja is the Jakob number of the fluid and c_l is the liquid thermal diffusivity and Pr is the liquid Prandtl number. The exponent to the Jakob number is estimated using various bubble growth experiments done independently [Zeng et al., 1993a, 1993b; Michaie et al., 2017; Pasquini et al., 2014; Kim et al., 2017; Goel et al., 2017]. The formulation is established on a particular portion of the data [Klausner et al., 1993; Michaie et al., 2017] while its predictions were tested on another set [Klausner et al., 1993; Michaie et al., 2017; Pasquini et al., 2014; Kim et al., 2017; Goel et al., 2017]. For subcooled boiling an additional subcooling factor (χ) is also multiplied to the growth rate. This incorporates the condensation due to the subcooled region.

3.3 Force Balance Model

Zeng et al. [1993] modelled the bubble force dynamics for pool boiling using the primary forces like surface tension, buoyancy, contact force, and the growth force. All these forces act in the direction normal to the surface in pool boiling. This force balance model is used, and the lift force on the bubble due to other bubbles is eliminated here assuming only a single bubble at the nucleation site at any specific time instant.

$$F_b = \frac{4}{3} \pi R^3 g (\rho_l - \rho_v) \quad (5)$$

$$F_s = d_w \sigma \pi \sin(\alpha) \quad (6)$$

$$F_g = \rho_l \pi R^2 (10R_1^2 + RR_2) \quad (7)$$

$$F_c = \frac{\pi \sigma d_w^2}{r_r} \quad (8)$$

$$\sum F_y = F_s + F_b + F_g + F_c \quad (9)$$

Where, R , R_1 , and R_2 correspond to the bubble radius as a function of time, the first derivative of R , and second derivative of R with respect to time, respectively. 'Lift-off' denotes the movement of the bubble normal to the heater surface. By resolving the forces acting on the bubble, if $F_y > 0$ implies bubble lift-off or departs from the nucleation site. More detailed discussion for the forces are provided by Mazzocco et al. [2018]

4. Results and Discussions

The goal of the present study is to understand boiling on a ultra-thin strip that has varying cross-sections. Experiments were performed on a nichrome strip to generate distinct, steadily forming bubbles, at the different cross-sections, i.e. on regions A and B as shown in the Figure 1b. Sections 4.1, 4.2 and 4.3 discuss in detail the results obtained from these experiments, while the predictions of the departure diameter model are discussed in Section 4.4.

4.1 General trend of bubble growth

The first goal is to visualise bubbles growing at gauge (A) and notch (B), and then to characterise how their growth varies from each other. It was observed that two bubbles of different sizes were generated. One bubble formed consistently at the notch, and another usually larger bubble, formed at the gauge. Continuous bubbles were observed to form and depart at each of these natural nucleation sites. In fact, burn marks representing

the bubble base diameter appeared on the specimen due to the high heat transfer achieved at the contact line of the bubble. These burn marks at the notch and gauge locations are shown in the Figures 1d and 1e, respectively.

When power is applied to a strip of varying cross-section, the different cross-sections experience different heat fluxes, as indicated in Figure 1c. The reduced cross-sectional area at the notch leads to higher heat flux compared to the gauge section. This results in a higher wall superheat at the notch, and thus smaller bubbles are formed, which grow quickly and depart earlier. The dominant forces that govern bubble departure are: (a) surface tension force that holds the bubble to the wall, (b) the growth force, and (c) the buoyancy force, which tends to pull the bubble away from the wall. A fine balance between these three forces usually exists and plays a role in the bubble departure. Since the wall superheat is high at the notch, the nucleating bubble starts growing quickly. Surface tension is small initially, and with the bubble growing quickly, the growth and buoyancy forces together are able to quickly overcome the surface tension force, resulting in the notch bubble's early departure.

For the gauge location, heat flux is lesser, hence growth force is lesser. The surface tension is able to keep up with the growth force and buoyancy force. Hence departure occurs at a much later stage, and when the bubble is bigger. Thus, smaller, faster growing bubbles are observed at the notch, and larger, slower growing bubbles are observed at the gauge. This is the general trend. However, this mode of growth or departure diameter can be changed if the surface texture/roughness were different. This will be demonstrated in the following sections.

4.2 Effect of subcooling on bubble growth

In this section, the bubble growth variation with subcooling is presented. The growth of a single bubble at the notch is visualized and shown in Figure 2a. The operating conditions were an input heat flux of 0.35 W/mm² at the notch, and a subcooling of 28.6 K, 38.6 K, and 43.9 K. Figure 2b shows bubble growth at the gauge. As stated by Mikic et al. [1970], bubble growth has two phases: inertia controlled growth followed by heat diffusion controlled growth. The inertia controlled growth phase is too fast to be captured by the present camera; the initial bubble size that can be captured is when the bubble growth starts to slow down i.e., when it transitions to heat-diffusion controlled growth. Thus, in this paper, the initial bubble size refers to the smallest bubble size that could be captured by the camera and not the nucleation size. The last image of each series shows the bubble at its departure size.

A plot of bubble diameter with time, at the notch, for various subcooled conditions is shown in Figure 3a. The growth rates of the bubble for low subcooling are more or less similar. Nevertheless, for highly subcooled conditions > 40 K, the growth rate and initial bubble size decrease significantly in comparison to the low subcooled conditions. The drop in initial bubble size is more significant than the reduction in growth rate. For different subcooling, it was observed that there is a difference in the initial and final diameter of the bubbles. This difference can be explained as follows. A lower degree of subcooling promotes vigorous inertia controlled growth, which results in the formation of larger initial bubbles. The reduction of liquid bulk temperature (increased degree of subcooling) impedes the growth during inertia controlled growth phase and leads to the formation of smaller initial bubbles, as shown in Figure 3a.

The departure diameter of the bubble (or maximum diameter observed during the growth period) also shows significant variation with subcooling. It is observed that the larger the initial bubble size at the end of the inertia controlled growth phase, the smaller is its heat diffusion controlled growth phase; the bubble departs earlier and at a larger size. This is evident specifically for the cases where the subcooling is low i.e., 28.6 K and 38.6 K, where the growth rates are almost identical; by the initial bubble size being different, their final diameter is also different. A larger initial bubble (for the 28.6 K bulk subcooling case) implies the buoyancy and growth force quickly overcomes the surface tension force, much earlier on, compared to the 38.6 K case. This highlights importantly, the interdependency between the initial and final bubble diameter. For the high subcooling case, one does see that the growth rate during the heat diffusion controlled phase is slightly slower, as the bulk is largely subcooled. The growth being slow results in lower growth force, and since the initial size is significantly small, the buoyancy and growth force takes a long time to overcome the surface tension force. A similar qualitative analysis holds valid for the bubble characteristics observed at the gauge location.

A different nichrome strip was taken to demonstrate the effect of a slightly different roughness/surface texture. Two strips of different surface roughness parameters were used. The measured roughness parameters for strip 1 are Ra - 181.50nm, Rq - 229.50nm, Rz - 916.33nm, and for strip2

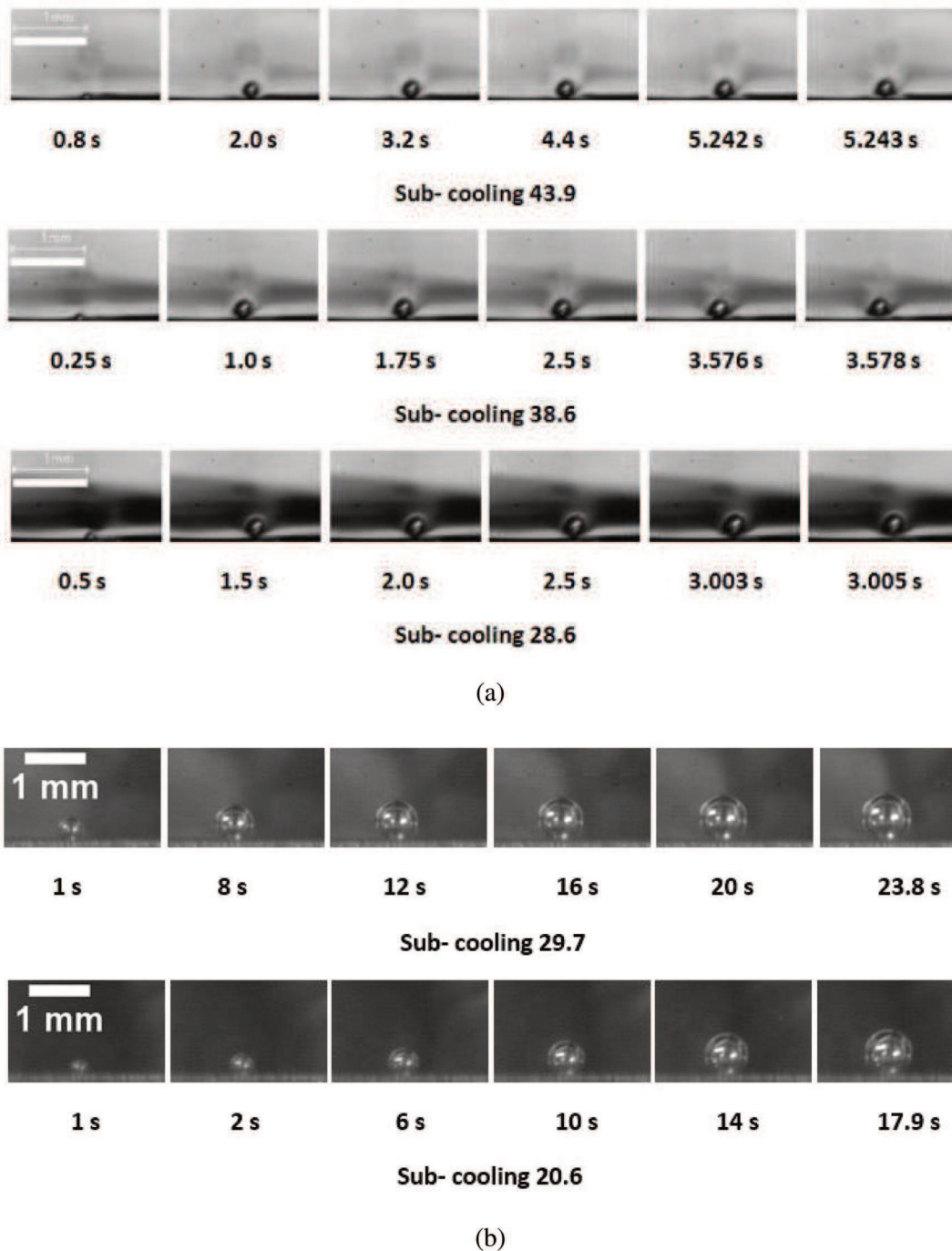


Figure 2: Bubble dynamics visualisation at various subcooling conditions over (a) notch and (b) gauge locations of the test strip.

are: R_a - 172.33 nm, R_q - 209.83 nm, R_z - 537.33 nm. This was measured using Alicona - Surface Profilometer. These almost similar roughness parameters indicate the significant influence of the notch on the bubble formation rather than the surface texture.

Where the bubble took approximately 4 s to grow (for 0.35 W/mm^2) on strip 1, on the new strip, it took 800 s to grow (for 0.30 W/mm^2). Their maximum sizes, however, were comparable i.e., 0.51 mm and 0.66 mm respectively. In fact, the bubble did not depart from the new strip and was stationary for a long time. This implies that the surface tension force is large for the new strip which significantly delayed the growth of the bubble. Thus, notch bubbles whose departure is usually very rapid can be considerably delayed due to surface roughness effect.

4.3 Effect of notch on bubble growth

Considering that both bubbles are formed on the same strip (same roughness along the strip), it could be expected that the notch and gauge would nucleate similar bubbles if the same heat fluxes were provided to each of them. To investigate this, two sets of experiments were performed. First, particular heat flux was maintained at the notch and the single bubble nucleating there was studied. Following this, the same heat flux was now applied to the gauge and the bubble generated at the gauge location was observed. This constitutes one experiment. Two such experiments were performed for two bulk temperatures (329 K & 309 K) with their schematic representation in Figures 4a and 4b

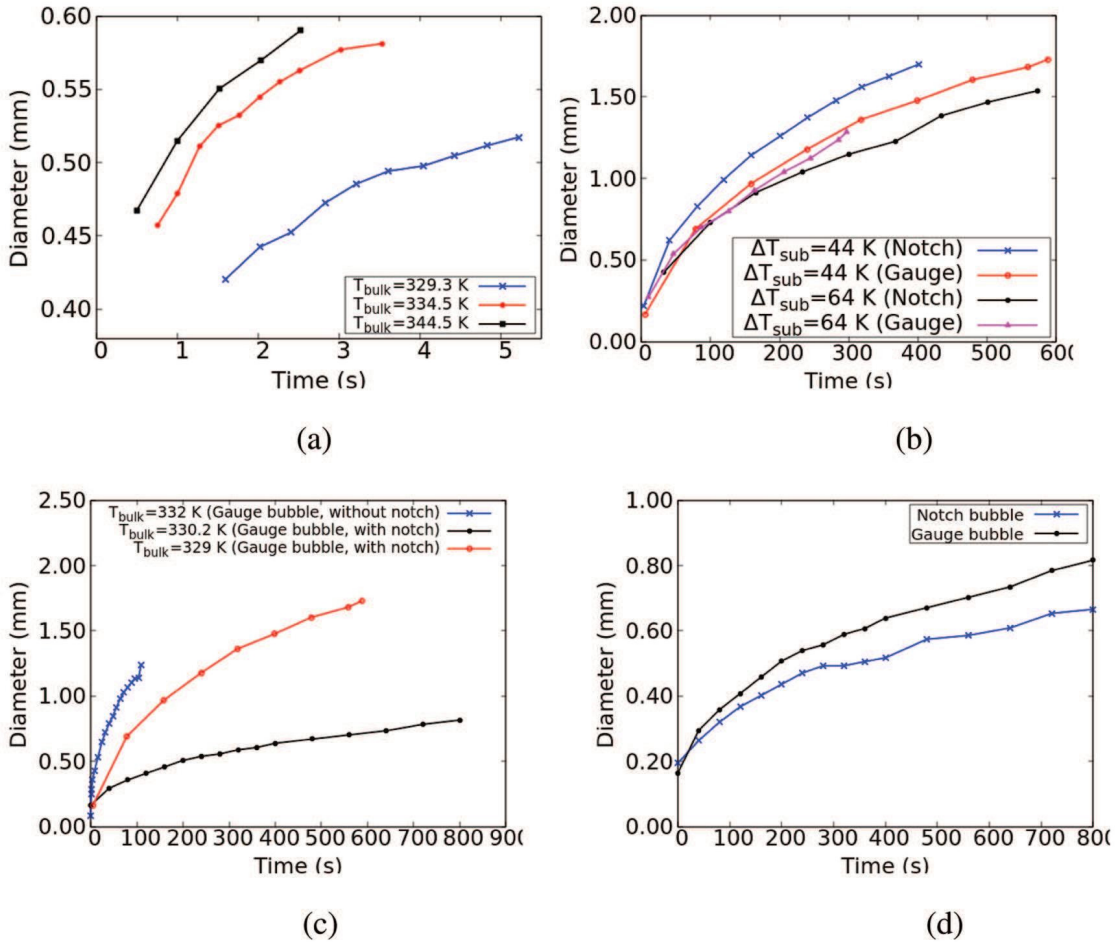


Figure 3: Plot of bubble growth at (a) notch location using test strip 1, (b) under same wall heat flux and different subcooling at notch and gauge (c) over gauge section of various surface roughness strips (strip 1, strip 2 and a strip without notch) (d) difference in bubble growth for notch bubble (notch heat flux = 0.30 W/mm^2 and gauge heat flux = 0.07 W/mm^2) and gauge bubble (notch heat flux = 0.7 W/mm^2 and gauge heat flux = 0.154 W/mm^2).

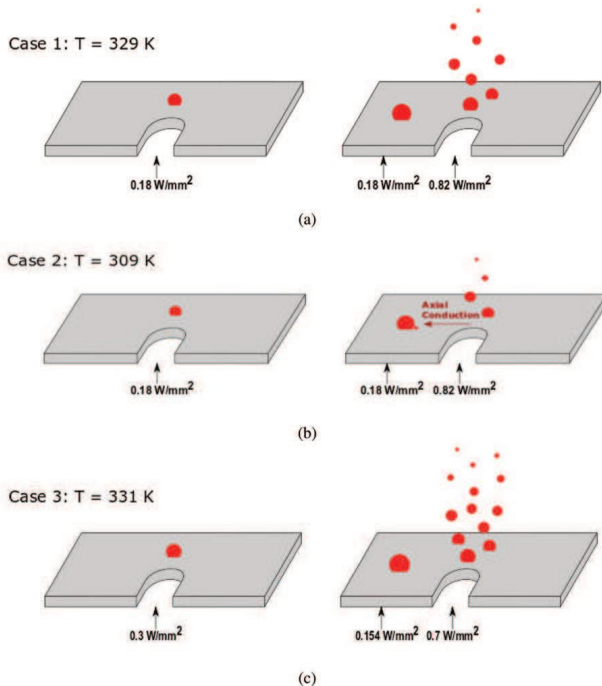


Figure 4: Schematic representation of bubble nucleation over notch and gauge for (a) for same heat flux conditions at $T_{\text{bulk}} = 329 \text{ K}$, (b) same heat flux conditions at $T_{\text{bulk}} = 309 \text{ K}$ and (c) different heat flux at $T_{\text{bulk}} = 331 \text{ K}$.

Case 1: The experiment was performed with a bulk temperature of 329 K . For this condition, a heat flux of 0.18 W/mm^2 was required to nucleate a bubble at the notch. The bubble also nucleates at the gauge when the same heat flux of 0.18 W/mm^2 is applied at the gauge. Though the same heat flux is applied, the growth rate of the bubble at gauge is lesser. This can be attributed to the fact that when the heat flux at the gauge is increased to 0.18 W/mm^2 , the corresponding heat flux at the notch becomes 0.82 W/mm^2 . This, along with the high bulk temperature, leads to vigorous boiling at the notch. The disturbance created by this vigorous boiling lowers the temperature within the superheated layer (SHL), as indicated in Figure 5a, and thus causes slower growth at the gauge. It needs to be pointed out here that the increased heat flux at the notch can sometimes result in axial conduction from notch towards the gauge. This is not too apparent in this case, as vigorous boiling at notch effectively removes heat from the notch, but in case 2, this becomes apparent.

Case 2: The bulk liquid temperature was reduced to 309 K . For this case, the bubble nucleated at the notch and the gauge at 0.18 W/mm^2 . However, the departure size of the bubble at the gauge is smaller than that for case 1, as shown in Figure 3b. Along with the bubble at the gauge, a smaller (assist) bubble formed under the “shade” of the gauge bubble, and assisted in its departure by nudging it. This was an interesting observation that was unique to Case 2. This can be explained as follows. When the heat flux of 0.18 W/mm^2 is at the gauge, the notch heat flux is 0.82 W/mm^2 , and several bubbles are usually forming at the notch. This was observed for Case 1. In Case 2, however, due to the bulk being highly subcooled, repeated bubbling was not observed at the notch. Hence, significant disturbance of the SHL, and cooling of the heater surface at the notch, did not take place. Due to very little nucleation at the notch, the wall temperature at the notch becomes high and results in axial conduction from the notch to the gauge. This result in the formation of a

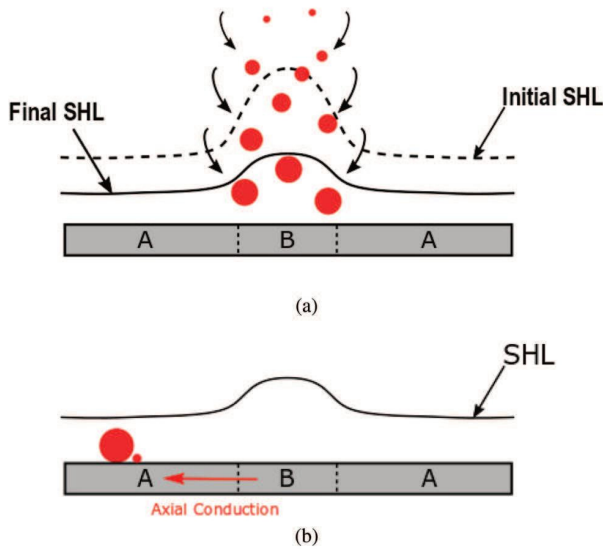


Figure 5: Schematic representation showing (a) thinning of superheated layer and (b) assist bubble formed over the strip with direction of axial conduction.

gauge bubble, as well as smaller assist bubbles at the gauge. The smaller assist bubble departed quickly, and while rising, nudged the bigger bubble forcing it to depart earlier, as shown in Figure 5b. It is to be noted here that the growth rate of the bubble at gauge is same as that of Case 1, though the bulk is cooler. This supports the theory that some amount of heat is flowing in from notch to gauge via axial conduction.

In section 4.2, it was mentioned that the roughness could alter the general boiling tendencies. This was demonstrated in section 4.2 by showing how departure could be delayed. Here we will look at how different roughness can change the effect of the notch on bubble growth. From case 1 and 2 discussed above, it was shown that the presence of notch decreases the growth rate of the bubble at gauge compared to notch. However, here, we will demonstrate how using another strip of a slightly different surface characteristic can result in the reversal of growth rates.

With this new strip, for the bulk temperature of 331 K, a heat flux of 0.30 W/mm^2 was required to generate a single bubble at the notch location. However, just previously, it was demonstrated that for a bulk of 329 K, 0.18 W/mm^2 was enough to nucleate a bubble (Figure 4a). This is most likely due to the difference in the roughness and cavity sizes of the respective strips. It is also observed that the higher heat flux case also has a lower bubble growth rate, as shown in Figure 3d. This is possible only if the surface tension at the surface of the strip is high.

Logically, similar to previous cases, it was expected that the initial nucleation of bubble at the gauge would also be for a heat flux of 0.30 W/mm^2 . But during experimentation, a much lower heat flux of 0.154 W/mm^2 was sufficient to nucleate a bubble at the gauge. This can be attributed only to the fact that when the heat flux at the gauge is increased to 0.154 W/mm^2 , the corresponding heat flux at the notch becomes 0.7 W/mm^2 . This, along with high bulk temperature leads to vigorous boiling at the notch. The mixing created by this vigorous boiling brings down the SHL temperature. While at the notch, with no mixing, a heat flux of 0.30 W/mm^2 was required for nucleation, one wonders how, at the gauge, with a reduction in SHL temperature due to mixing, nucleation occurs at 0.154 W/mm^2 . This is possible only if axial conduction plays a role in raising the temperature near gauge so that the bubble is able to nucleate at 0.154 W/mm^2 itself, as shown in Figure 4c. The different surface texture also results in slower growth than previous cases.

An experiment is carried out on strips, with and without the notch. This showed that mostly, the presence of notch slows the bubble growth at the gauge, as shown in Figure 3c.

4.4 Model Predictions

The model developed in this paper was intended towards predicting bubble departure for wide range of subcooled pool boiling cases. This model has been tested on different experimental datasets of pool boiling of water, both from literature, as well as, with the data generated in the

present study:

- Klausner et al. [1993]: Saturated at 2.76 and 1.93 Bar for a constant wall superheat of 10 K at the saturation temperature of 392.4 K and 403.85 K respectively. [8 Data Points]
- Kim et al. [2017]: Saturated at 1 Bar for wall superheat ranging from 4.5-10.6 K. [5 Data Points]
- Michaie et al. [2017]: Saturated at low pressure ranging from 0.042-0.2 Bar and wall superheat ranging from 8.82-13.37 K at a constant heat flux of 27 W/mm^2 . [58 Data Points]
- Pasquini et al. [2014]: Sub-cooled at 1 Bar for various low subcooling temperatures ranging from 0.8-7.8 K and a heat flux of $55-910 \text{ W/mm}^2$. [25 Data Points]
- Present study: High subcooling from 20 to 65 K for a moderate heat flux from $64-95 \text{ W/mm}^2$. [35 Data Points]

Figure 6a shows the performance of the present departure diameter model over the whole spectrum of pool boiling datasets. Very high subcooled pool boiling data is not available in the literature, and experiments performed in the present study (green dots in Figure 6a) provide this much needed data. The bubble departure diameter model's predictions have been compared against it. The model predicts well for saturated boiling conditions, with a large number of predictions falling under 40% deviation. Most of the predictions for low subcooling data fall within 40-80% deviation. There is an equal scatter of about 60% for the deviations of high subcooling data. These error percentages across the wide range of subcooling are better than the performances of other models previously discussed in the literature review section.

During the development of the departure diameter model, it was observed that the bubble growth model plays a key role in the predictions. Initially, the bubble growth force was modelled using the popular bubble growth models. The predictions however did not capture well the high

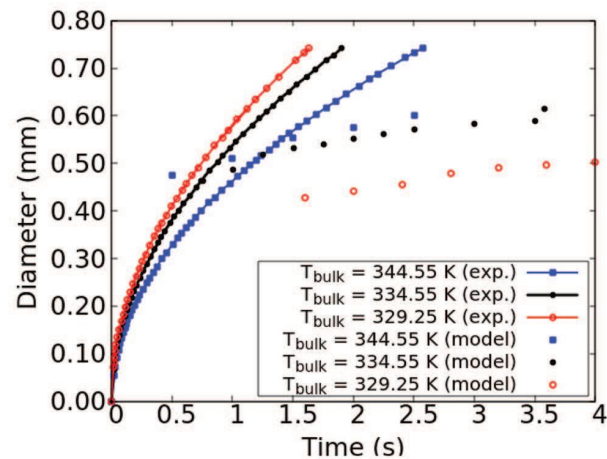
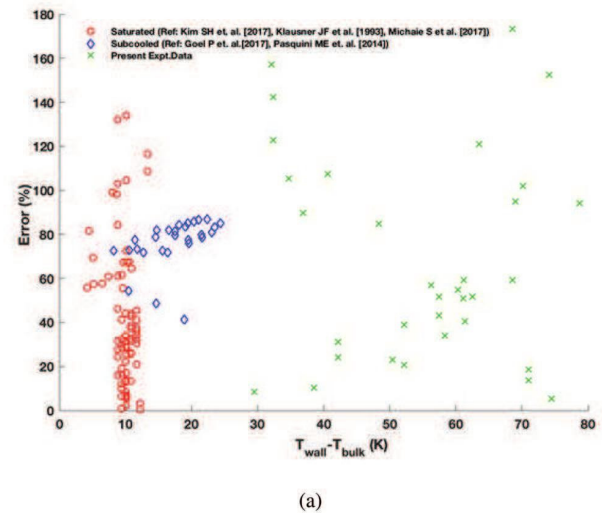


Figure 6: Plot showing the (a) departure diameter prediction for pool boiling using present model and (b) growth prediction of smaller bubble.

subcooled conditions. Thus, a modified bubbled growth model was introduced, which improved the predictions of the departure diameter model across the spectrum of the saturated and subcooled datasets. The subcooling effect was incorporated using a multiplier, and indeed it improved the predictions. However, it can be seen below that the present bubble growth model is not ideal. Its predictions differ from what is observed in the experiments of this present study. These are discussed more in detail below.

Experiments show that with increasing bulk temperature, the initial bubble size is higher. This implies that inertia controlled growth is more rapid when the bulk is hotter. From Figure 6b, it is observed that the heat diffusion controlled growth phase is similar in most cases. Now, in looking at the model predictions, it is concluded that the model differs significantly from the experiments. First, looking at the initial bubble size prediction, it is observed that the growth model under-predicts initial bubble size for low subcooling cases, and slowly transitions to over-predicting the initial bubble size for high subcooling cases. Thus, it is clear that the subcooling effect on inertia controlled growth is not accurately captured by the model. For hotter bulk, it has to grow faster, while for colder bulk it has to grow slower. In looking at the model, it can be seen that the growth model proposed in this paper has a $Ja^{2.1}$ power dependence, wherein Jakob number is directly proportional to the superheat temperature. This implies that the growth rate is higher if the wall temperature is much higher than the saturation temperature. This however, did not account for the bulk temperature aiding in bubble growth. Only the bulk effect currently accounted for is the variation in fluid properties due to the bulk temperature and the subcooling multiplier. But clearly, these parameters do not capture the effect wherein the near-wall fluid actually behaves as a supplier of heat to the bubble interface. Thus, a modification to the subcooling parameter is required.

After the initial bubble size is reached, the bubble undergoes heat diffusion controlled growth. Even here, the model over-predicts all the growth rates significantly. And, as observed earlier, deviation/over-prediction is more for highly subcooled liquid. In heat diffusion controlled growth, the effect of bulk is bound to be more dominant since the upper interface of the bubble moves closer to the cooler bulk. However, the bulk effect is not accurately captured, as can be seen in Figure 6b. Consequently, the trend between model and experiments differ, wherein the model predicts much higher growth than experiments. This high growth rate predictions impacts the prediction of the departure diameter of the bubbles. A higher growth rate causes bubbles to grow quickly and to a much larger size. Similar predictions are observed at the notch and gauge location. In fact, the model predicts best for the hottest bulk where there is the least effect of subcooling. Modifications are currently underway to incorporate the subcooling effect more effectively. These modifications will also account for the variation in bulk temperature between the notch and gauge locations, as well.

5. Conclusions

Pool Boiling on ultra-thin strips with varying cross-section was studied. Experiments were performed for a wide range of subcooling, wherein micro-scale visualisation of the bubble growth and departure was systematically recorded and analysed. The following observations were made regarding the bubbles growing at the wider cross-section (gauge), and the narrow cross-section (notch) of the ultra-thin strip:

1. The presence of notch slows growth on the strip in all locations other than the notch. At the notch, smaller, faster bubbles are formed while at the gauge, a larger bubble is formed.
2. Subcooling affects growth rates in both locations. The initial bubble size governs bubble departure. The forces due to bubble growth and surface tension play a significant role in the departure, but the effect of initial bubble size appears most dominant.
3. Low subcooling can cause bubble crowding at the notch, and probably an early onset of CHF.
4. For high subcooling, bubble crowding at notch does not exist. In this case, axial conduction sets in from notch to gauge location, and causes assist bubbles to form near the gauge bubbles. The presence of these assist bubbles destabilises the gauge bubbles and results in them departing quickly at a smaller size. Thus, effective heat transfer is not achieved both at the gauge and the notch.

5. Using a strip with higher roughness slows bubble growth considerably at the notch. Thus, using a strip with appropriate roughness could prevent bubble crowding at the notch, and could facilitate axial conduction to set in between notch and gauge locations. If the axial conduction is moderate and not excessive, then a higher bubble growth will occur at the gauge without assist bubbles impeding heat transfer. Thus one concludes that optimum subcooling needs to be ensured. Significant importance must be given to choosing an optimal subcooling in combination with the strip roughness to ensure efficient heat transfer from the strip.

The study also presents a preliminary departure diameter model, which indicates improved bubble departure prediction capabilities across a wide range of subcooling.

References

- [1] Dhillon NS, Buongiorno J, Varanasi KK, 2015, Critical heat flux maxima during boiling crisis on textured surfaces, *Nature communications*, 6, 8247
- [2] Duan X, Phillips B, McKrell T, Buongiorno J, 2013, Synchronized high-speed video, infrared thermometry, and particle image velocimetry data for validation of interface-tracking simulations of nucleate boiling phenomena, *Experimental Heat Transfer*, 26, 169-197
- [3] Giraud F, Rullière R, Toubanc C, Clausse M, Bonjour J, 2015 Experimental evidence of a new regime for boiling of water at subatmospheric pressure, *Experimental Thermal and Fluid Science*, 60, 45-53
- [4] Goel P, Nayak AK, Kulkarni PP, Joshi JB, 2017, Experimental study on bubble departure characteristics in subcooled nucleate pool boiling, *International Journal of Multiphase Flow*, 89, 163-176
- [5] Gupta S, Navaraj WT, Lorenzelli L, Dahiya R, 2018, Ultra-thin chips for high-performance flexible electronics, *NPJ Flexible Electronics*, 2, 8
- [6] Hao W, Xiao-Feng P, Christopher DM, 2005, Dynamic bubble behaviour during microscale subcooled boiling, *Chinese Physics Letters*, 22, 2881-2884
- [7] Judd RL, Merte H, and Ulucakli ME, 1991, Variation of superheat with subcooling in nucleate pool boiling, *Journal of heat transfer*, 113, 201-208
- [8] Kim SH, Lee GC, Kang JY, Moriyama K, Park HS. and Kim MH, 2017. The role of surface energy in heterogeneous bubble growth on ideal surface, *International Journal of Heat and Mass Transfer*, 108, 1901-1909
- [9] Kim SM, Mudawar I, 2014, Review of databases and predictive methods for heat transfer in condensing and boiling mini/micro-channel flows, *International Journal of Heat and Mass Transfer*, 77, 627-652
- [10] Klausner JF, Mei R, Bernhard DM, and Zeng LZ, 1993, Vapor bubble departure in forced convection boiling, *International journal of heat and mass transfer*, 36, 651-662
- [11] Kowalewski TA, Pakleza J, Chalfen JB, Duluc MC, Cybulski A, 2000, Visualization of vapor bubble growth, In 9th International symposium on flow visualization, 176-1
- [12] Liang G, Mudawar I, 2019, Review of single-phase and two-phase nanofluid heat transfer in macro-channels and micro-channels, *International Journal of Heat and Mass Transfer*, 136, 324-354
- [13] Lu JF, Peng XF, 2006, Bubble leaping and slipping during subcooled boiling on thin wires. *International journal of thermal sciences*, 45, 908-916
- [14] Mazzocco T, Ambrosini W, Kommajosyula R and Baglietto E, 2018, A reassessed model for mechanistic prediction of bubble departure and lift off diameters, *International Journal of Heat and Mass Transfer*, 117, 119-124
- [15] Michale S, Rullière R, Bonjour J, 2017, Experimental study of bubble dynamics of isolated bubbles in water pool boiling at subatmospheric pressures, *Experimental Thermal and Fluid Science*, 87, 117-128
- [16] Mikic BB, Rohsenow WM, Griffith P, 1970, On bubble growth rates, *International Journal of Heat and Mass Transfer*, 13, 657-666
- [17] Pasquini ME, Cariteau B, Josserand C, Salvatore P, 2014, Experimental study on subcooled nucleate boiling from a single artificial cavity, 10th International Conference on Heat Transfer, Fluid Mechanics and Thermodynamics
- [18] Shen B, Suroto BJ, Hirabayashi S, Yamada M, Hidaka S, Kohno M, Takahashi K and Takata Y, 2015, Bubble activation from a hydrophobic spot at "negative" surface superheats in subcooled boiling, *Applied Thermal Engineering*, 88, 230-236
- [19] Sugrue R, Buongiorno J, McKrell T, 2014, An experimental study of bubble departure diameter in subcooled flow boiling including the effects of orientation angle, subcooling, mass flux, heat flux, and pressure, *Nuclear Engineering and Design*, 279, 182-188
- [20] Zeng LZ, Klausner JF, Bernhard DM, Mei R, 1993, A unified model for the prediction of bubble detachment diameters in boiling systems, *Flow boiling*, *International journal of heat and mass transfer*, 36, 2271-2279